Z-99 SECONDARY MIGRATION IN A 2D VISUAL LABORATORY MODEL

F. VASSENDEN [1,2], Ø. SYLTA[1], C. ZWACH[3]
[1] *SINTEF Petroleum Research, NO-7465 Trondheim, Norway.*
[2] *Now at Statoil.*
[3] *Norsk Hydro.*

Abstract

Reservoirs and cap-rocks undergo burial during geological time. Hydrocarbons migrate into and fill traps during periods of active expulsion from source rocks. The supply of oil and gas can be abundant until deep burial stops the supply. Capillary leakage of oil and gas from the trap can then potentially decrease the size of the accumulation. A laboratory study of filling into and leakage out of a trap has been undertaken with a visual 2D laboratory model. The model defined a synthetic cap rock having a finite entry pressure overlying a permeable reservoir rock. The trap was formed by imbedding a pyramid-shaped layer of smaller glass beads in a pack of larger glass beads.

During migration of oil into the trap, the oil column in the trap was found to build up to an entry column height, at which leakage through the seal started. A steady state oil filling level was observed at a maximum column height slightly higher than the entry height. When the oil supply to the trap was stopped, the trap emptied to 35% of the entry column height. By repeated filling, no leakage occurred until the oil level reached the original entry level. The emptying of the trap to 35% was also repeated.

The behaviour is explained quantitatively by a theory of capillary snap-off, based on the geometry of the pore space in the glass bead pack. With no adjustable parameters, the theory predicts the oil column after leakage to be 32% of the oil entry column height, in reasonable agreement with the observations. The snap-off phenomenon can be embedded in relative permeability and capillary pressure curves for the seal. With such rock curves, the trap emptying dynamics was quantitatively reproduced by a theory with one adjustable parameter.

The presented theories conceptually explain the filling state of a real trap after a general migration supply history. Quantitative predictions should also be possible if the seal is sufficiently well characterized.

Introduction

Petroleum exploration is often performed with the Gussow fill-spill concept (Gussow, 1954). The burial history of source rocks normally makes heavy hydrocarbons the first to be expelled from the source rock, followed by lighter and lighter hydrocarbons. Hydrocarbons fill traps down to the spill point, and surplus hydrocarbons will spill over to neighbouring traps in the

same geological unit. A consequence of this is that lighter hydrocarbons (gas) should preferentially fill traps near the source, and force oil to be spilled into shallower traps (Gussow, 1954). Therefore, oil traps should typically be discovered further away from the basin axes than gas filled traps.

An alternative approach includes static capillary properties of cap-rocks (Berg, 1981). Berg (1981) defined a static sealing column of a cap-rock from the cap-rock entry pressure (that can be measured) divided by gravity times the density contrast between water and the hydrocarbon phase:

$$h_e = \frac{p_e}{\Delta\rho g} \qquad (1)$$

When the static sealing column is greater than the structural closure height, hydrocarbon will spill from one trap to the next in the manner described by Gussow (1954), i.e., laterally within the geological unit. In contrast, if the sealing column is less than the closure height, then this analysis leads to the conclusion that all hydrocarbons that migrate out of the trap will leak up through the cap-rock. The cap rock entry pressure analysis therefore often results in hydrocarbon system interpretations that focus migration within basin centers. The same source can fill several vertically stacked traps, e.g. Jurassic and Tertiary traps. The capillary leakage process described by Berg (1981) implies that the light hydrocarbons would be expected to occur in shallower exploration targets and the heavier oil near the source rock. This is opposite of the sorting obtained in systems controlled by the fill-spill process.

The dynamics of oil flow in the sealing rocks does not play any role in the determination of the sealing properties of the traps in the static assessment. If the seals of traps have dynamic flow properties (see e.g. Sylta, 2002), flow may be directed both laterally through their spill point and vertically through their cap rock seal at the same time, leading to different migration scenarios than the static case.

In this work we aim to investigate these problems by controlled laboratory experiments. The question addressed in this paper is the behaviour of the oil after a capillary controlled breakthrough of oil through a seal has occurred. Possible hypotheses are that the oil would reach a steady state during filling of the trap (maintaining the static fill of sealing column), or that the trap would be emptied completely upon breakthrough. The behaviour after the oil supply stops is also addressed, with possible hypotheses being that the oil level would stay fixed at its maximum level, be somewhat reduced, or reduced to zero. The relevance of these questions for the understanding of the oil distribution in exploration targets is obvious from the above.

In this study, a capillary entry pressure trap was therefore constructed in a 2D visual model in order to discern between these different hypotheses. Quantitative models based on pore geometries were constructed in order to explain the trap drainage dynamics and the residual filling after drainage.

Experimental

2D visual model

The 2D visual model used here was described by Holt and Vassenden (1996). One application of it was discussed by Holt and Vassenden (1997). A sketch of the flow apparatus is shown in Figure 1. The porous medium is kept between two glass plates that fit in a frame of solid

polyoxymethylene strengthened by stainless steel. The inside measures of the frame is 47 by 67 cm.

The model was packed by pouring glass beads in between the glass plates through dedicated filling ports along the top of the model. First, 200-300 µm glass beads were filled through the left filling port. The heap formed looked like a regular pyramid, with the sides tilting at their critical slope (26.8°). This zone constituted the reservoir. Then, 70-110 µm beads were poured onto the pyramid to form a 6.5 cm thick layer of even thickness on top of the reservoir zone, and this constituted the capillary seal. The remaining volume of the model was filled with 200-300 µm beads through both filling ports on top. The bead-pack was compacted by exerting a force on the glass plates while the model was vibrated.

The inlet and outlet sides of the model were each equipped with 16 independent flow ports. Fluids (solvents for cleaning, water for initialization, and oil for the migration experiments) were injected into the flow model by use of two eight channel peristaltic pumps (Gilson Minipuls 3). Oil was injected in a single port, located just below the capillary seal. Several of the ports located in the water zone, both above and below the seal and on both sides of the model, were coupled to a liquid reservoir (separator) near the model. In the migration experiments, the reservoir was filled with the same aqueous equilibrium phase as the 2D model (discussed below). A near-hydrostatic pressure distribution was thus ensured in the water zone during the experiments. The absolute pressure was slightly above atmospheric, in order to avoid the formation of air bubbles. The overpressure was obtained by letting the effluent from the reservoir flow to a beaker located 1.5 m above the model.

The bead pack was illuminated from behind, while photo- and video cameras were placed in the front of the flow model.

The properties of the bead pack are presented in Table 1. The permeabilities and porosities of each porous medium were measured when the 2D model was filled completely with one type of beads. It cannot be guaranteed that precisely the same parameters apply to the different porous media when mixed in one pack.

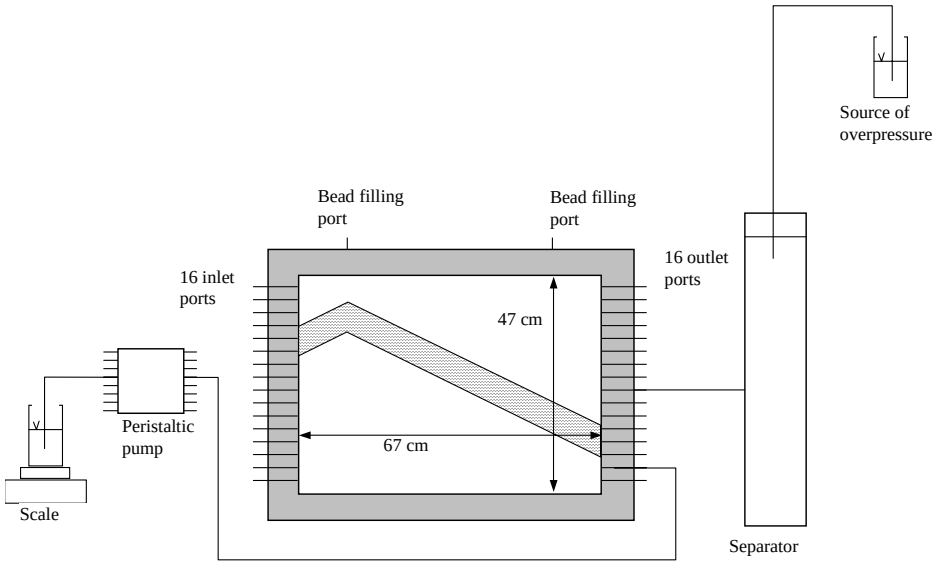

Figure 1 The 2D flow apparatus

Table 1 Porous medium properties.

	Entire inhomogeneous bead pack	Seal material	Reservoir material
Length, cm	67		
Height, cm	47		
Width, cm	1.047±0.026		
Bead size, µm	-	70-110	200-300
Permeability, D	58 [1)]	4 [2)]	72 [3)]
Porosity, fraction	-	0.38 [2)]	0.35±0.01 [4)]

[1)] Effective permeability measured during flow from left to right, with injection and production occurring over the entire height of the model.
[2)] From Holt and Vassenden 1997
[3)] Estimated from pressure drop and rate measured during water injection of homogeneous bead pack
[4)] From model geometry, the mass of glass beads, and a measured glass density of 2.487±0.005 g/ml.

Capillary properties of seal material

The seal material was characterized by a direct measurement of the entry pressure in an air-water porous plate experiment. A layer of 70-110 µm beads formed the porous plate for a pack of 200-300 µm beads packed in a tube. The porous medium was filled with fresh water at ambient conditions, and air was injected at known pressure. The air pressure was increased step-wise until air broke through the layer of 70-110 µm beads. This occurred at an overpressure in the air (relative to water) of 113 mbar. The interfacial tension of the air-water system is tabulated at 72 mN/m.

Fluid system

The requirement that gravity-driven entering of the oil into the seal should be obtained, given the physical dimensions of the model and the entry pressure of the capillary seal, dictated the choice of fluid system to be used in the experiments. The requirement for a useful fluid system is that the interfacial tension and density difference fulfils

$$\frac{\sigma}{\Delta\rho g h_e} = \frac{\sigma_{aw}}{p_e^{aw}} \qquad (2)$$

with a practical value of the entry height, h_e. Schechter et al (1991) have presented a three-component system based on iso-octane (iC8), iso-propanol (IPA), and brine (water with 2 wt% $CaCl_2$), which are completely miscible for some compositions, and exhibits two liquid phases for other compositions. The interfacial tension between the two liquid phases can be varied continuously from 38.1 mN/m for the mixture between iC8 and brine to zero at the critical point. The density difference varies along with the interfacial tension. Therefore, by choosing the composition of this ternary system, the ratio between interfacial tension and density difference could be tuned, and a system designed with the desired level of oil filling when oil enters the cap-rock. The two phases were made by mixing components at the mass fractions given in Table 2, and letting the equilibrated phases segregate in a separating funnel. The oil and water phases formed were dyed with Sudan red (40 mg/l) and disulfine blue (10 mg/l), respectively. The interfacial tension was measured with a Krüss ring tensiometer, and the densities were measured with an Anton Paar oscillating tube densiometer. The obtained properties are listed in Table 2.

Table 2 Ternary mixture composition and properties of equilibrium phases at 20°C

Composition	Volume fraction	Mass fraction
IPA (iso-propanol)	0.2758	0.25347
iC8 (iso-octane)	0.3000	0.24289
brine (2 wt% $CaCl_2$)	0.4242	0.50364
σ	2.94	mN/m
ρ_w	958.6	kg/m^3
ρ_o	697.6	kg/m^3
$\Delta\rho$	261	kg/m^3

Injection program

After packing, the 2D model was first saturated with distilled water. Water was displaced by the aqueous equilibrium phase (water phase) before the experiment. Three cycles of oil injection were carried out, with the conditions shown in Table 3. The oil injected was the oleic phase produced by the mixture shown in Table 2.

Table 3 Experimental injection conditions

Experiment	Injection rate, ml/h	Initial condition	Actions during experiment
A	54	Saturated with aqueous equilibrium phase	Un-dyed oil injected. Trap allowed to empty to steady state level during shut-in period. Remaining oil displaced from trap through seal by water phase flooding
B	5.13	Trap and seal exposed to un-dyed oil. Trap empty	Red oil injected. Trap allowed to empty to steady state level during shut-in period.
C	5.13	Trap and seal exposed to red oil. Some red oil in trap.	Red oil injected. Trap allowed to empty to steady state level during shut-in period

It was difficult to obtain sufficiently accurate volumetric data for high-rate injection of un-dyed oil, experiment A. Therefore, volumetric data and pictures presented are from the low-rate experiments B and C. The initial condition and saturation history differed for all three cycles, as shown in Table 3.

Results

Qualitative discussion

Figure 2 shows selected examples from a series of images taken during the first low-rate injection cycle, experiment B. The timing and the characteristics of the different frames are summarized in Table 4. The first four frames of Figure 2 illustrate the growth of an oil zone in the trap. The migrating oil finger has just reached the top of the trap in the first frame, and the accumulation of oil has just started. The second frame shows the trap half-full. Oil had just been detected above the trap at the time of the third frame. This oil had leaked through the

capillary seal at the crest of the trap, as revealed by red oil traces in the seal. These traces are not easily discerned from the colour images, but are clearly seen in the difference images shown in Figure 3 (discussed below). At the time of frame 4, oil injection was stopped. The oil level in the trap increased somewhat between the time of entering (frames 3) and the near-steady state shown in frame 4 (the measured oil level is given in Table 4). This level increased is referred to as over-filling below.

After the oil supply was stopped, the oil column shrunk, as shown by frames 4-6 of Figure 2. Frame 5 was taken shortly after the injection was stopped, and frame 6 at the end of Experiment B. The oil column height is nearly static in frame 6, and very close to the minimum value observed. The static nature of this state was not positively proven over the limited duration of Experiment B. In Experiment C, however, this static state was found to prevail for as long as the experiment lasted and several months after the data collection were stopped.

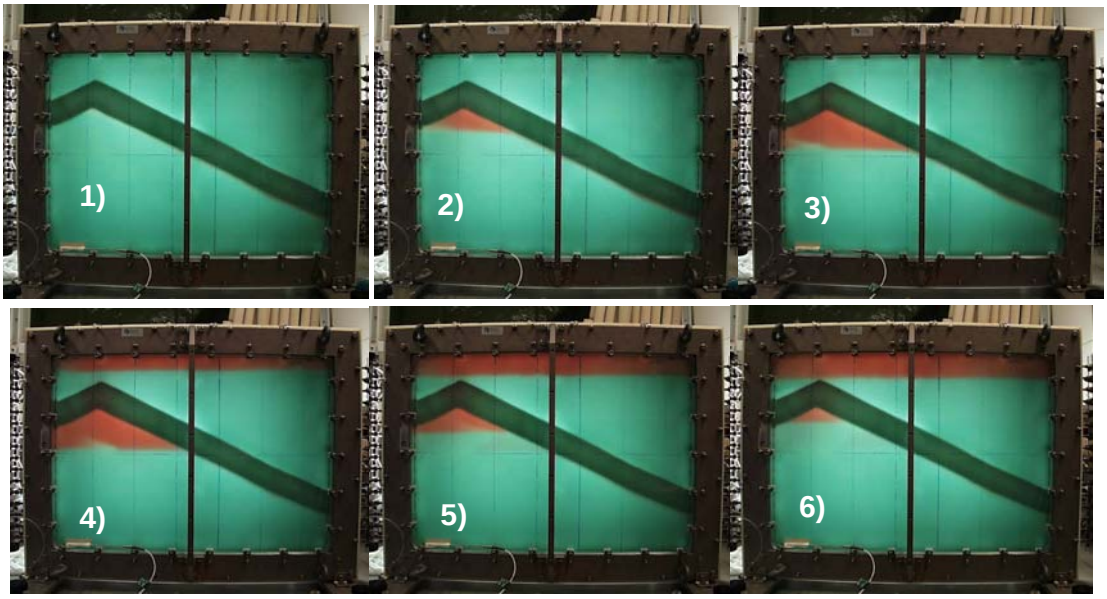

Figure 2 The first slow oil injection, experiment B. Frame numbers are explained in Table 4.

Figure 3 presents difference images, calculated as the difference between the blue channels of each image and the blue channel of the image taken before oil injection. The migrating oil finger below the cap rock is seen in these images. The two first frames show absence of oil above the trap. Frame 3 reveals the first oil detected above the trap, and the oil path through the shale layer. This path is most strongly developed in frame 4, which was taken at the end of oil injection. Flow through the seal occurred in a diffuse region about 11 cm wide. In frames 5 and 6, the oil finger along the seal has shrunk somewhat after oil injection ceased, and the oil column in the trap has become smaller.

Figure 4 shows difference image 6 with contrast enhancement and with lines and arrows highlighting the interesting zones observed. Arrows point at the oil-water contact prevailing at the time of the picture, and at the deepest OWC observed before the injection of oil was stopped. A shade of colouring between the two levels indicate the presence of residual oil in the water-invaded zone. The two vertical lines indicate the outer boundaries of observations of oil in the seal, and mark the occurrence of residual oil in the area of leakage flow.

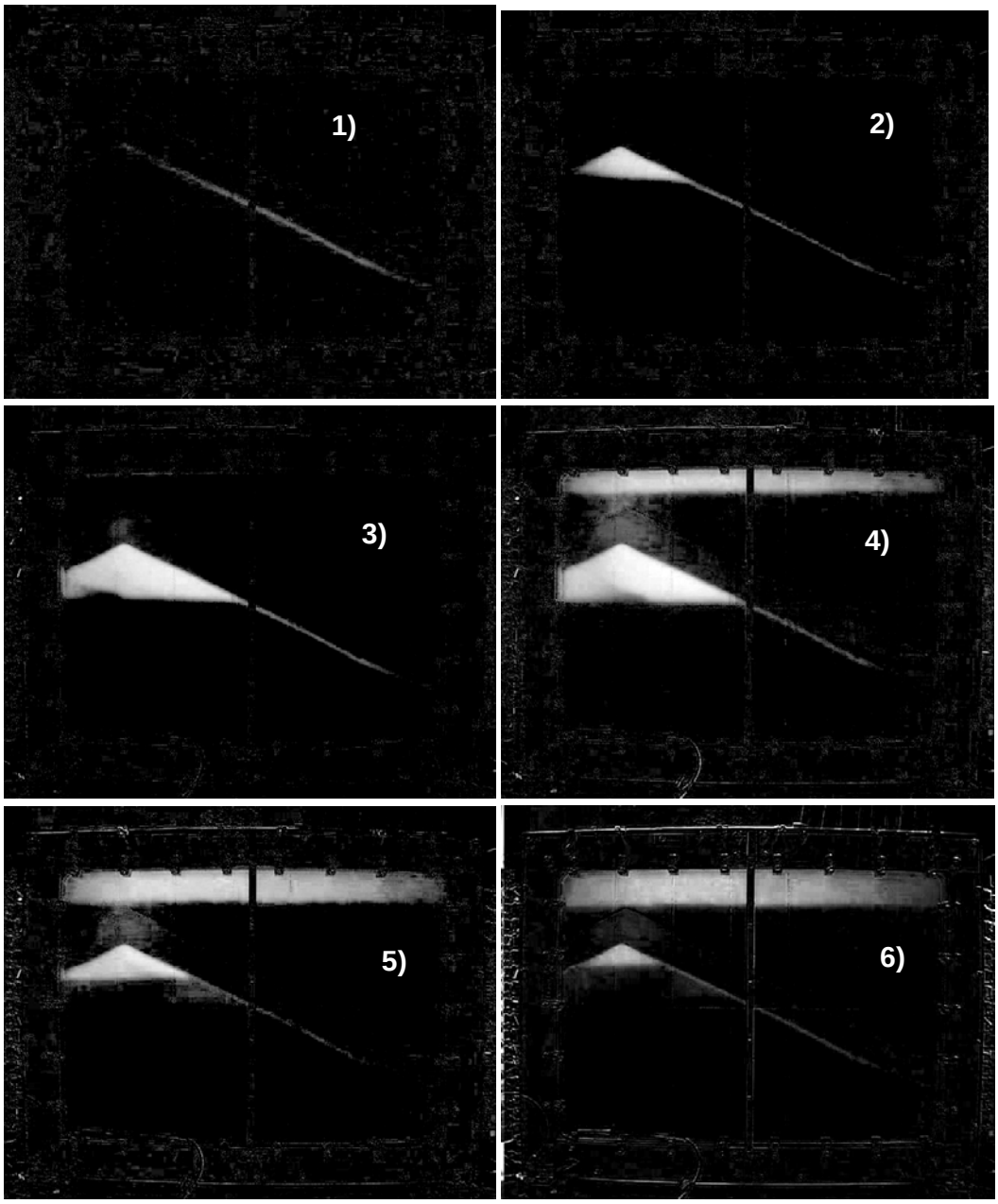

Figure 3 Difference images from the first slow oil injection experiment, experiment B (at the times in Table 4).

Table 4 Timing of images presented and summary of column heights for the images shown in Figure 2.

Frame	Time h	Injected volume ml rock	Oil level in trap cm	Oil level above trap cm	Comment
1	0.8	10	1.2	0.0	oil finger reaches trap
2	4.6	60	5.6	0.0	trap half filled
3	13	175	9.9	0.3	first oil above trap
4	29	376	10.2	3.4	oil injection stopped
5	44	376	6.0	4.9	half empty
6	309	376	3.7	5.8	minimum level

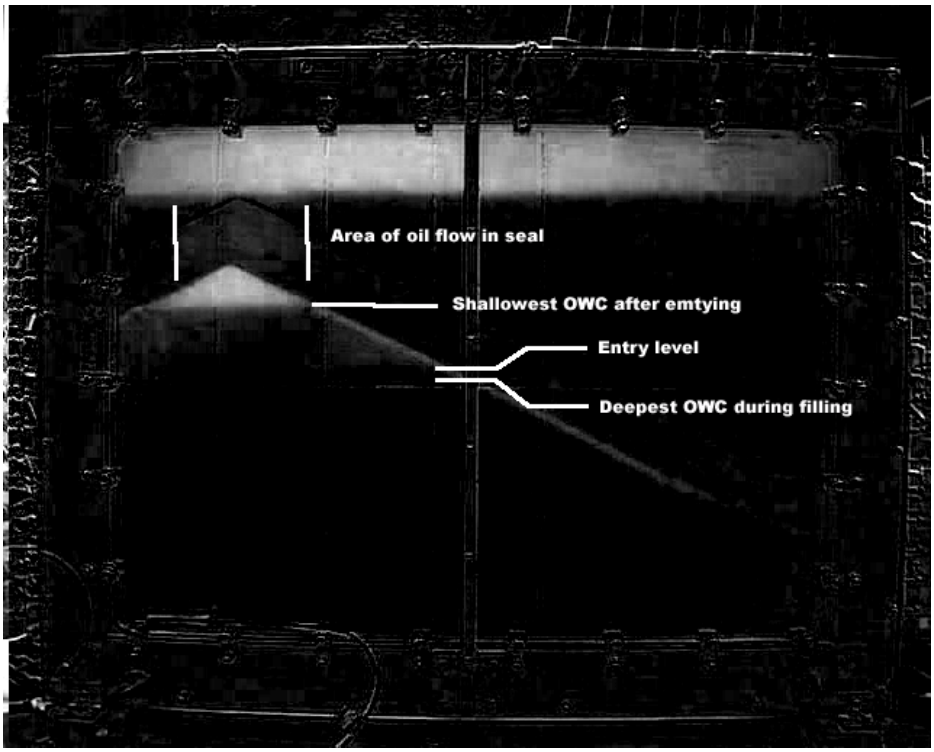

Figure 4 Difference picture for the last time-step shown in Figure 3, highlighting the different zones observed.

Volumetric analysis

The volumetric measurement for the slow oil injection experiments were made on the digital images, using image-processing software (Adobe Photoshop) to read off the thickness of the oil zones below and above the seal. Despite the existence of a 9 mm thick capillary transition zone between oil and water, readouts were reproducible with average measurement noise of 1.3 mm. The volume of oil in the model was estimated from the measured oil zone dimensions, the bead pack thickness, porosity, and the residual water saturation in the oil zone, S_{wi}, which was found to have a value close to zero, in order to ensure a match between the oil volume injected and the volume detected in the model by image analysis.

The development of the oil column height through the low-rate cycles (B and C) is shown in Figure 5. The response in the two cycles was essentially identical. The late data of experiment C was omitted for clarity in Figure 5. The detailed variation of the oil level during filling and emptying of the trap is discussed in the following.

Figure 6 details the oil level variation during filling of the trap. Initially, there is a delay in the filling of the cell, corresponding to the time required for the oil finger to propagate from the injection port to the top of the trap. Thereafter, the trap is found to fill according to the geometry of the trap and the assumption of no leakage (solid line), until leakage through the seal begins. Leakage is proven by the observation of oil above the trap. With oil leakage, the oil column height levels off, and reaches a steady state. Table 5 summarises the observed column heights. The entry column heights are similar for experiment B and C. The steady state filling during injection shows a small difference, with a 0.5 cm over-filling of the trap (steady state filling over the level defined by the entry pressure) for experiment B, and 0.8 cm for experiment C.

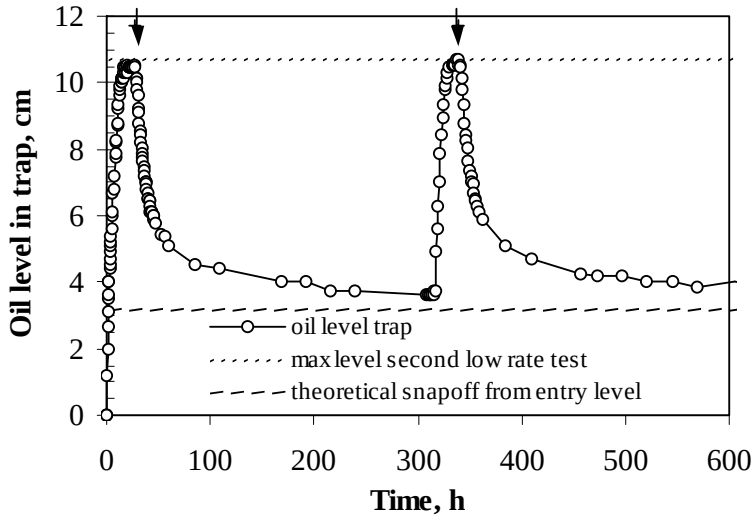

Figure 5 Oil level variations through the low-rate experiments. Arrows indicate the end of oil injections. The snap off level is discussed in the text.

The over-filling in steady-state is believed to be governed by a balance between oil inflow rate and seal transport properties. Exactly at the entry pressure, only one pore (the largest) is filled with oil. If the injection rate is larger than the transport capacity of this pore, additional pores have to be entered, until the capacity matches the injection rate. The additional pores opened could be both smaller pores at the top of the trap and pores located further down on the seal structure. In both cases, the filling level must increase relative to the entering level, in order to supply the additional capillary pressure required to enter new pores. The reason for the difference in over-filling between the two low-rate experiments is not known.

Table 5 Column heights in the three injection cycles.

Experiment	A	B	C
Breakthrough oil column, cm	7	10	9.9
Maximum oil column, cm	11	10.5	10.7
Shut-in period, h	20	290	786
Final oil column, cm	5	3.7	3.7

In experiment A, entry occurred at a much lower column height, and steady state was found at a higher column height than in the low-rate experiments. The early entering is probably due to the viscous pressure drop over the seal due to the too rapid injection. The larger over-filling is a direct consequence of the higher oil injection rate.

A very important observation was made during the filling period of experiment C (not shown in the figure): The leakage of oil through the seal did not start until the oil level was approximately equal to the breakthrough column height in experiment B. This is noteworthy because oil had been leaking out of the trap the entire shut-in period of experiment B, and one could suspect still-open flow paths to resume leakage as soon as injection in experiment C started. The experiment proved otherwise: No (or immeasurable few) flow channels were open to flow at the end of the experiment B shut-in. The same entry pressure had to be overcome in order for oil to enter the seal the second time as the first time.

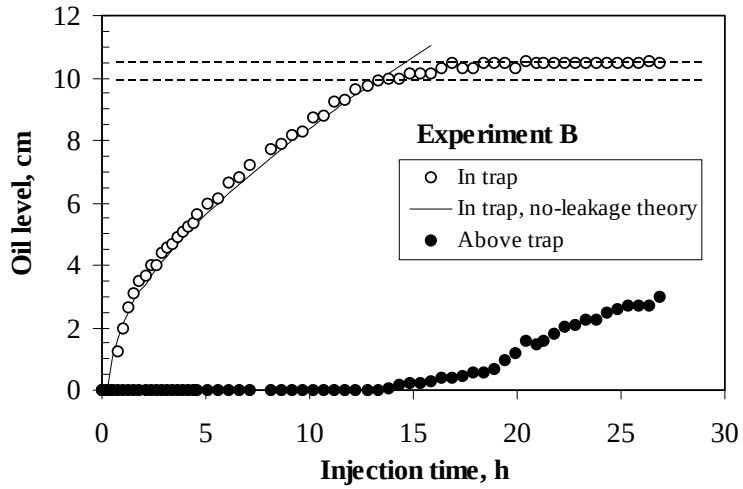

Figure 6 Details of the oil column build-up during the first low-rate injection cycle. The dashed lines show the oil levels at breakthrough and at steady state.

Figure 7 illustrates the long term behavior of the oil column during trap drainage. The figure clearly proves that the low degree of filling observed after a long period of trap emptying in fact is a true static state. A static state at 3.7 cm filling can be inferred for the last cycle. This corresponds to 35 % of the oil column observed when oil first entered the seal.

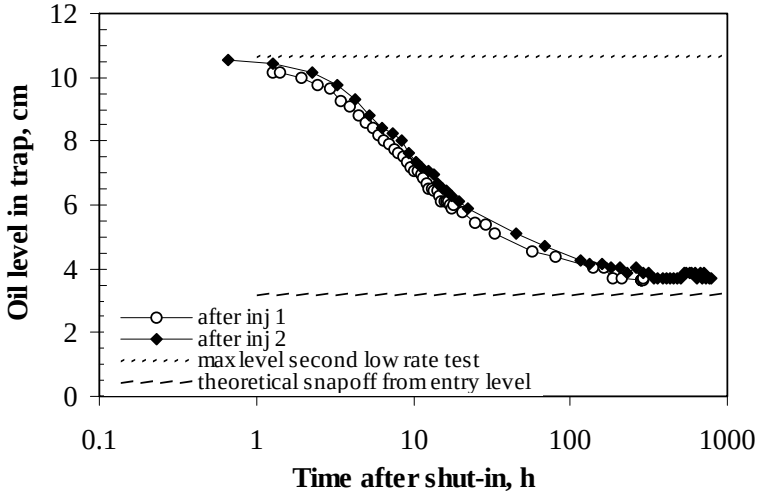

Figure 7 The oil rate variation during shut-in, plotted with a logarithmic time scale.

The most important observations made in the capillary trap filling and emptying experiments are

- entering of oil, and start of leakage through the seal, at well-defined column height.
- steady state at slight over-filling attained during injection
- reduction to 35% of entering column after stop of oil supply.
- the 35% column height is a truly stable state.
- repeated injection cycles experience the same entry column height as the first cycle.

Theoretical interpretation

Snap-off theory

The observed behaviour of the trap filling and draining can be understood on the basis of pore level phenomena. Figure 8 illustrates an oil finger entering a pore in the seal during filling (increasing p_c) and emptying of the trap (decreasing p_c). The model pore has the shape of a triangular prism. The capillary pressure (equivalent to the trap filling level) relates to the interface curvature in two principal directions (r_1 and r_2) through the Young-Laplace equation (see e.g. Adamson, 1990)

$$p_e = \frac{\sigma}{r_1} + \frac{\sigma}{r_2} \qquad (3)$$

At entering, the tip of the finger is shaped like a hemisphere, with two equal curvatures. The largest hemisphere fitting into the pore has the radius of the inscribed circle of the pore cross-section, r_i. This defines the entry pressure of the pore (Roof (1970), Ransohoff and Radke (1988), Falls et *al.* (1989)). After entering, oil can flow through the pore, and cause leakage out of the trap. When the trap empties, p_c decreases, and water fill the corners of the flow channel. Also at this lower p_c, oil can flow in the pore. When the curvature radius r equals the inscribed circle radius r_i , a capillary instability is initiated, however. Any fluctuation that accumulates some water will cause the curvature radius to increase, and the resulting increase in capillary pressure will cause the further accumulation of water at that location. This is a so-called snap-off process that causes the oil finger to break into droplets. In a general flow channel with variable cross-sectional dimensions, snap-off will make the oil immobile. Snap-off in the triangular prism occur at a snap-off capillary pressure, $p_s=p_e/2$.

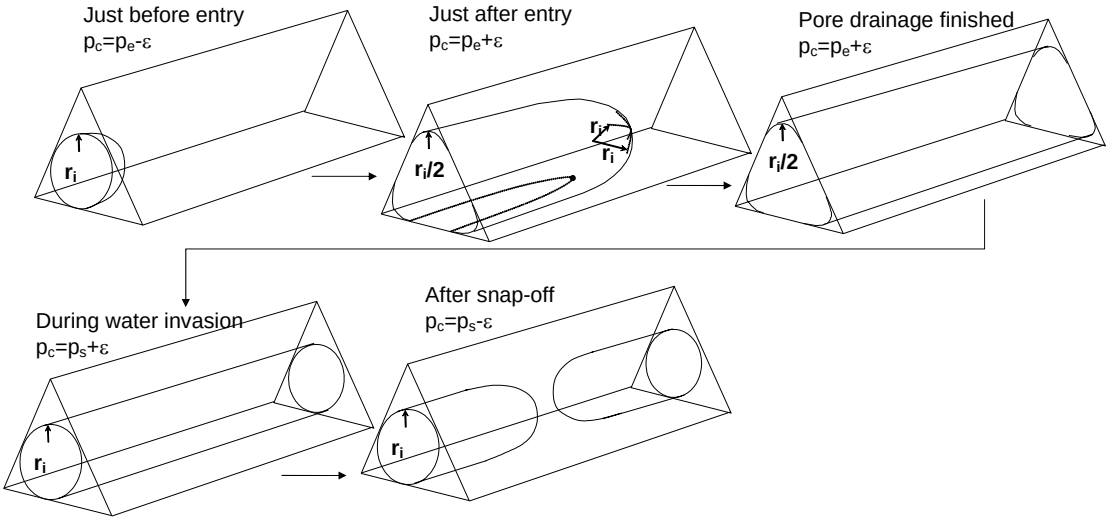

Figure 8 Oil finger in a triangular pore

In the glass bead pack used in the experimental study, the tetrahedral configuration of beads shown in Figure 9 is expected to be abundant. Such clusters of beads contain pore throats formed by three contacting beads. Triangular pore throats will be found frequently also in a random pack of glass beads such as our 2D model. In the random bead back, also larger pores and throats exist, as revealed by the additional porosity found in the random bead pack compared to the tightest pack of spheres (0.35 for the 2D model vs. 0.26 for the tightest packing of equal spheres (Ashcroft and Mermin, 1976)). If the larger pores are too few to be connected, triangular throats may still control transport of fluids in the medium, however.

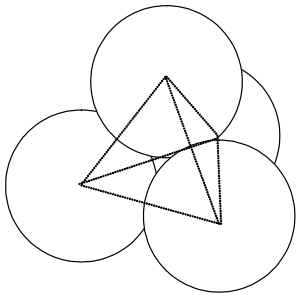

Figure 9 Tetrahedral cluster of spheres in the tightest packing of equal spheres.

Snap-off analysis for a pore throat between three glass beads is more complicated, but the arguments are the same as for the triangular prism. Firstly, the entry pressure is still determined by the largest hemisphere that can be contained between the three beads, and the entry pressure is still described by Equation (3). After entering, the interface in the throat is pressed into the corners between the beads, and the water forms a pendular ring around the contact points between each pair of spheres (Falls *et al.,* 1989). This is illustrated in Figure 10. The pendular ring corresponds to the corner water in the prismatic pore, but the interface shape is more complicated, as it is characterized by two different curvature radii, r_c and r_p. Here, r_c is the radius of the meniscus in the plane of drawing in Figure 10, and r_p is the radius around an axis normal to the plane of bead contact.

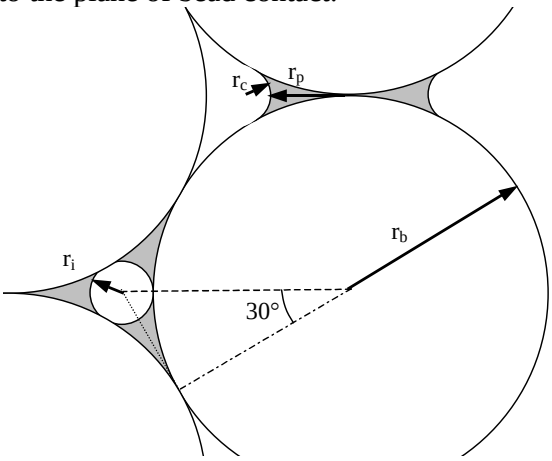

Figure 10 The pendular ring of water at the contact between two spheres and the inscribed circle, with construction aids.

The capillary pressure is defined as the overpressure in the non-wetting phase due to interface curvature. This implies that the radius r_c describes a positive curvature, $1/ r_c$. The interface curves towards the phase with the highest pressure, just like a balloon curves towards high-pressure air. In contrast, the radius r_p describes an interface that curves away from the non-wetting phase. This curvature reduces the pressure in the non-wetting phase, and therefore the curvature due to the radius r_p is counted as negative, $-1/ r_p$.

The snap-off criterion can be formulated the same way for the bead pack as in the prismatic pore. The criterion is that snap-off occurs when the menisci from the three corners meet, which is when $r_c=r_i$. That occurs at a snap-off capillary pressure of

$$p_s = \sigma\left(\frac{1}{r_i} - \frac{1}{r_p}\right) \qquad (4)$$

Table 6 presents snap-off pressures for several pore geometries. Some of the entry and snap-off pressure values are the same as presented by Falls et al. (1988). The configuration with two beads at the wall is included since it may arise as an experimental complication in the 2D experiments. The square pore throat is found in octahedral clusters in the tightest pack of beads. The triangular prism provides an upper limit for the snap-off/entry pressure ratio, but is also a good approximation of long, straight pores typically formed at contacts with non-spherical grains, and in pores narrowed by diagenesis. Thus it may be that the snap-off/entry pressure ratio of real cap rock approaches 0.5. For a given rock, a microscopic investigation of the pore structure can provide the exact value.

Table 6 Characteristics for three different pore geometries (bead radius r_b is length unit)

	r_i/r_b	r_p/r_b	p_e/σ	p_s/σ	p_s/p_e
Triangular prism *)	*1*		*2*	*1*	*0.5*
Triangular	0.158	0.423	12.9	4.10	0.317
Wall & 2 beads **)	0.25	0.5	8	2	0.25
Square **)	0.414	0.586	4.83	0.707	0.146

*) bead size has no meaning for triangular prism, use units of r_i instead.

Interpretation of experiments in view of snap-off theory

In the 2D model experiment, where the entry oil column height was 10 and 9.9 cm at oil entry (for the two low-rate cycles, see Table 3), triangular pore throats are predicted to have snap off column heights at 3.17 and 3.14 cm, respectively, from the snap-off/entry pressure ratio presented in Table 6. For a theory with no adjustable parameters, this is in reasonable agreement with the observed column height of 3.7 cm after prolonged shut-in. It therefore appears that the snap-off theory provides a reasonable explanation for the static oil column observed long after the oil supply stopped. Several effects may account for the slight deviation, the most important being that the glass beads used have a distribution of sizes. Clearly, the wall pores, square pores and multiply bridged pore throats are not connected through the bead pack, or else the asymptotic filling level after drainage would be lower than predicted for the triangular pore throat.

Dynamics of emptying, a description with relative permeability and capillary pressure curves

While the snap-off theory provides a pore-level explanation for why the oil-water contact stops at a certain level during emptying of a trap, it is interesting to find out if the process can be described by the conventional reservoir engineering tools and concepts, relative permeability and capillary pressure (rock curves). It is particularly important to discuss if relative permeability and capillary pressure data measured with conventional methods for other purposes can be used to predict trap filling and emptying.

A model for the emptying of the trap after the end of injection can be constructed by assuming that oil is flowing through a cross-section A of the capillary seal, which has a thickness L. The thickness of the bead pack is w. The flow zone, having a width A/w in the images of the 2D model, can be seen particularly well in frame 4 of Figure 3, but it is not a sharply defined zone. The precise value does not matter in this model, however. The driving force for oil flow is the decrease in oil flow potential from below to above the capillary seal. Just above the capillary seal, we can assume that oil and water pressures are both equal to the water hydrostatic profile, neglecting the small capillary effects in the coarse-grained porous medium. The oil pressure just below the seal is $\Delta\rho gh$ higher than the hydrostatic water

pressure, where h is the thickness of the oil zone at the highest point of the trap. The driving force for flow is thus $\Delta\rho gh$. The Darcy law gives the flow, q_o, of oil through the shale layer as

$$q_o = \frac{Akk_{ro}(S_w)}{\mu_o}\frac{\Delta\rho gh}{L} \tag{5}$$

The saturation S_w is the water saturation in the oil flow zone in the seal. This saturation has to be consistent with the capillary pressure curve of the seal material:

$$S_w = p_c^{-1}(\Delta\rho gh) \tag{6}$$

If these equations are applied to the steady state oil injection rate, q_{oss}, and the resulting steady state column height, h_{ss}, a value can be found for the product $Ak_{ro}(S_w)$. I.e., the relative permeability for oil in the seal can be determined if the flow area is known, or vice versa. Equations (5) and (6) can be used to calculate the over-filling of the trap during injection. Several approximations are made in this simple derivation, the most prominent being that changes in capillary pressure and saturation through the seal material, and variation with flow are with oil column height is neglected.

Geometrical considerations of the trap pyramidal shape (with the sides of the trap having an angle θ to the horizontal) show how the oil rate flowing out of the trap relates to the rate of change of the oil level:

$$q_o = w\varphi(1-S_{wi})\frac{d}{dt}\left(\frac{h^2}{\tan\theta}\right) \tag{7}$$

Eqs. (5)-(7) define an ordinary differential equation describing how the oil column h varies with time during trap emptying. The detailed behaviour is determined by the shape of the functions $k_{ro}(S_w)$ and $p_c(S_w)$. A parameterization of the rock curves is required for the analytical solution of the differential equation to be possible. During emptying of the trap, the saturation in the seal varies from the steady state saturation found during oil injection, to the saturation where k_{ro} is zero. This saturation interval can be mapped on to the interval 0-1 for a variable x, and the relevant part of the imbibition k_{ro} and p_c functions can be quite generally be assumed to have the shapes:

$$k_{ro} = k_{ro}^{ss}(1-x)^{n_o} \tag{9}$$

$$p_c(x) = (p_{ss} - p_s)(1-x)^{\frac{1}{\lambda}} + p_s \tag{10}$$

where k_{ro}^{ss} and p_{ss} is the steady-state relative permeability and capillary pressure prevailing before the oil injection stopped, and p_s is the snap-off capillary pressure, where $k_{ro}=0$. The shapes of the employed capillary pressure and oil relative permeability curves are compared in Figure 11, on a completely arbitrary saturation axis selected just for the illustration.

In order to compare with the laboratory results, the capillary pressures can be expressed by quantities measured in the experiment as $p_{ss,s}=\Delta\rho gh_{ss,s}$. The steady state oil relative permeability during injection can likewise be calculated from Eq. (5) with the steady state oil injection rate q_{oss}. When Equations (5)-(10) are integrated, and the substitution of laboratory observables is carried out, one obtains for the time variation of the oil column during trap emptying:

$$\frac{h-h_s}{h_{ss}-h_s}=\left[1-t\frac{(1-\lambda n_o)\tan\theta q_{oss}}{2w\varphi(1-S_{wi})h_{ss}(h_{ss}-h_s)}\right]^{\frac{1}{1-\lambda n_o}} \quad (11)$$

This model has one free parameter, namely the product of the rock function exponents, λn_o. All other parameters are fixed by other aspects of the experiment than the emptying dynamics.

Table 7 Model parameters used in the calculation of trap emptying

Experimental observables, drainage dynamics			**Additional observables used to find level of k_{ro}**		
w	1.047	cm	A	11	cm^2
θ	26.8	°	μ	0.63	cP
φ	0.35		L	6.5	cm
q_o	5.14	ml/h	Δρ	261	kg/m^3
h_{ss}	10	cm	g	9.8	m/s^2
h_s	3.7	cm	k	4	D
Capillary pressure and relative permeability curve			λn_o	1.33	

The results of the calculations are shown in Figure 12. This figure compares the measured data from Experiment C, with theoretical curves for the oil level as a function of time. The curve labeled "Model fit" was calculated with Equation (11), with parameters given in Table 7, and the rock curves labeled "imbibition" in Figure 11. A good match was achieved after adjusting the λn_o product. The optimal value of this product was 1.34. In order to illustrate the sensitivity, the figure also shows curves calculated for values 0.5 and 2. These curves lie below and above the best match, respectively.

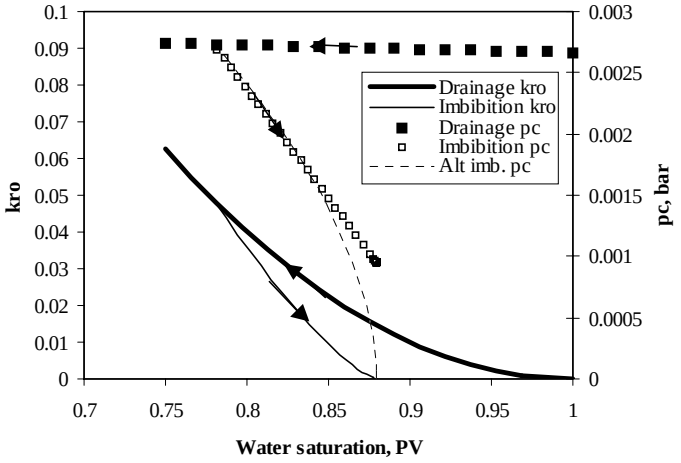

Figure 11 Rock curves used in the model for trap emptying. The drainage curves are only shown for illustration, and are not used in the calculations. The saturation interval spanned by the imbibition curves is completely arbitrary.

In addition to the rock curves giving a good match, Figure 11 also presents an alternative imbibition capillary pressure curve. The alternative capillary pressure curve is almost equal to the best match curve, except at the k_{ro}=0 saturation, where it has a zero value instead of a non-zero value. This alternative curve is what one normally would get from an imbibition capillary pressure measurement in a porous plate experiment, when the capillary pressure is decreased stepwise to zero. The point with p_c=0 would normally be measured by immersion in water, and one would conclude that p_c=0 when the fluids stop flowing. This is wrong when snap-off is active, however. At the snap-off capillary pressure, capillary continuity is lost, and the capillary pressure becomes poorly defined (in-fact, it is the condition k_{ro}=0 that stops the

fluids flowing). Figure 12 shows that the resulting rock curves predicts total trap emptying, in contrast to the observations. Conventionally measured capillary pressure data are therefore not applicable for the prediction of trap emptying.

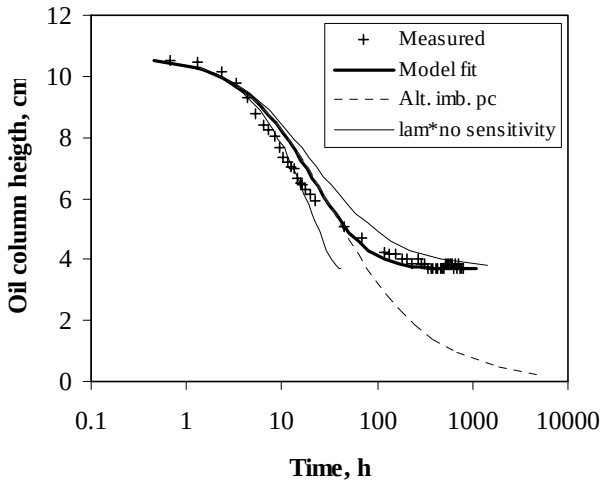

Figure 12 Calculated temporal development of the oil column during emptying compared to measured data from the second cycle of oil injection.

The good match between the measured and theoretical drainage dynamics data shows that a model based on capillary pressure and relative permeability curves for the seal can grasp the essentials of the experiment. The only requirement is that the rock curves reflect the capillary snap-off phenomenon, with the relative permeability to oil being zero at a non-zero capillary pressure.

Conclusions

The filling of and leakage out of a trap was studied with a visual 2D laboratory model. A reservoir and an overlying cap rock with different entry pressures were represented in the model by large and small glass beads. The trap was defined by a pyramid-shaped layer of smaller glass beads imbedded in a pack of larger glass beads.

The model was initially saturated with an aqueous phase, and an oil phase was injected below the cap rock layer. A model fluid system was specially designed for this experiment. The oil column in the trap was found to build up until the capillary pressure at the top of the trap exceeded the entry pressure of the cap rock. As long as oil supply to the trap continued, the column height was constant at a slight over-filling relative to the entry level. When the oil supply ceased, the trap emptied to 35% of the maximal column height. It was shown that this level represented a static state. When oil injection was resumed, the oil column build up to the original entry level before leakage through the seal started. The response in the second oil injection cycle was identical to the first cycle, in all respects.

The ratio between the entry and minimal column heights can be explained by a theory of capillary snap-off, based on the geometry of the pore space in the glass bead pack. With no adjustable parameters, this theory predicted the oil column after leakage to be 31% of the oil entry column height, in excellent agreement with the 35% observed. It was also shown that the dynamics of trap leakage could be explained with the concepts of relative permeability and capillary pressure curves, provided that the capillary pressure had a value larger than zero for the saturation where the oil relative permeability becomes zero. This condition is a way of describing the occurrence of snap-off with relative permeability and capillary pressure curves.

Thus, it has been shown that the 2D model experiment with leakage out of a capillary trap can be explained quantitatively with the snap-off theory. It was found that conventional imbibition capillary pressure experiments will not capture the crucial features that are required to predict the asymptotic filling level.

The experiments and the theory support the Berg (1981) notion of capillary controlled leakage out of hydrocarbon traps. The experiments have revealed the importance of dynamic processes (oil mobility within the seal) in controlling the steady state oil column during steady state oil influx. The experiments have clarified that traps do not empty completely due to capillary leakage, but rather attain a static partial filling at snap-off conditions long after the oil supply has stopped.

Acknowledgements

Norsk Hydro is acknowledged for funding and allowing the publication of this study, and Rolando di-Primio for assistance in the problem formulation. Torleif Holt and Kåre Solbakken are acknowledged for constructing the 2D visual model, during the RUTH research program. Oddmund Frigård and Arild Moen are acknowledged for technical assistance with packing of the model and experimental work.

References

ADAMSON, A.W. 1990: Physical Chemistry of Surfaces, 5th ed., John Wiley & Sons, New York.

ASHCROFT, N.W. and MERMIN, N.D., 1976: “Solid State Physics”, Saunders College, Philadelphia.

BERG, R. R. 1981: Calculation of seal capacity from porosity and permeability data. American Association of Petroleum Geologists Bulletin 65, 5, p.900.

FALLS, A.H., MUSTERS, J.J., and RATULOWSKI, J 1989: The Apparent Viscosity of Foams in Homogeneous Bead Packs, SPE Reservoir Engineering (May 1989) 155.

GUSSOW, W. C. 1954: Differential entrapment of oil and gas: A fundamental principle. American Association of Petroleum Geologists Bulletin 38, 5, 816-853.

HOLT, T., and VASSENDEN, F, 1997: “Reduced Gas/Water Segregation by Use of Foam”, 9th European Symposium on Improved Oil Recovery, 20-22 October 1997, The Hague

HOLT, T., VASSENDEN, F. 1996: Physical gas/water segregation model in RUTH 1992-1995 Program Summary, Norwegian Petroleum Directorate, Stavanger, 75-84.

LIDE, R. (ed) 1990: Handbook of chemistry and physics, 71st edition, CRC Press, Boston.

RANSOHOFF, T.C. and RADKE, C.J., 1988: Mechanisms of Foam Generation in Glass-Bead Packs, SPE Reservoir Engineering (May 1988) 573.

REID, R.C., PRAUSNITZ, J.M., and POLING, B.E:, 1988: “The properties of gases and liquids.” Chemical Engineering Series, McGraw-Hill Book Company, New York.

ROOF, J.G., 1970: “Snap-Off of Oil Droplets in Water-Wet Pores”, SPEJ March 1970, p 85, Transactions vol 249 (170)

SCHECHTER, D.S., ZHOU, D., and ORR, F.M. Jr., 1991: “Capillary imbibition and gravity segregation in low IFT systems”, presented at the 12th Workwhop and Symposium of the IEA Collaborative Project on Enhance Oil Recovery, Bath, England, October 28-30 1991.

SYLTA, Ø., 2002. Modelling techniques for hydrocarbon migration: Can we do better. Presentation at workshop, EAGE 64’th Conference & Exhibition, Florence 2002. Extended Abstract.